



The structure-based design, synthesis, and biological evaluation of DNA-binding amide linked bisintercalating bisanthrapyrazole anticancer compounds

Brian B. Hasinoff^{a,*}, Rui Zhang^a, Xing Wu^a, Lynn J. Guziec^b, Frank S. Guziec Jr.^b, Kyle Marshall^b, Jack C. Yalowich^c

^a Faculty of Pharmacy, University of Manitoba, 750 McDermot Avenue, Winnipeg, Manitoba, Canada R3E 0T5

^b Department of Chemistry and Biochemistry, Southwestern University, Georgetown, TX 78628, USA

^c Department of Pharmacology and Chemical Biology, University of Pittsburgh School of Medicine, Pittsburgh, PA 15261, USA

ARTICLE INFO

Article history:

Received 25 February 2009

Revised 28 April 2009

Accepted 30 April 2009

Available online 6 May 2009

Keywords:

Bisanthrapyrazole

Bisintercalating

DNA-binding

Topoisomerase II

ABSTRACT

A series of amide-coupled bisanthrapyrazole derivatives of 7-chloro-2-[2-[(2-hydroxyethyl)methylamino]ethyl]anthra[1,9-cd]pyrazol-6(2H)-one (AP9) were designed using molecular modeling and docking and synthesized in order to develop an anticancer drug that formed a strongly binding bisintercalation complex with DNA. Concentration dependency for the increase in the DNA melting temperature was used to determine the DNA binding strength and whether bisintercalation occurred for the newly synthesized analogs. The ability of the compounds to inhibit the growth of the human erythro-leukemic K562 cell line and inhibit the decatenation activity of DNA topoisomerase II α was also measured. Finally, the compounds were evaluated for their ability to act as topoisomerase II poisons by measuring the topoisomerase II α -mediated double strand cleavage of DNA. All of the bisanthrapyrazoles inhibited K562 cell growth and topoisomerase II α in the low micromolar range. Compounds with either two or three methylene linkers formed bisintercalation complexes with DNA and bound as strongly as, or more strongly than, doxorubicin. In conclusion, a novel group of amide-coupled bisintercalating anthrapyrazole compounds were designed, synthesized, and evaluated for their physico-chemical and biologic properties as potential anticancer agents.

© 2009 Elsevier Ltd. All rights reserved.

1. Introduction

Some of the most efficacious anticancer drugs bind to DNA and in doing so inhibit DNA topoisomerase II (EC 5.99.1.3) which results in cell growth inhibition and/or cell death. Included among these drugs are the anthracyclines such as doxorubicin and daunorubicin, and amsacrine, and mitoxantrone.¹ These planar aromatic molecules intercalate into DNA and promote DNA strand breaks through their interaction with DNA topoisomerase II.¹ Because the clinical use of doxorubicin and the other anthracyclines is limited by the development of a cumulative dose-dependent and potentially fatal cardiotoxicity, which is likely due to oxidative stress on the relatively unprotected cardiac muscle, non-cardiotoxic topoisomerase II-targeted anticancer drugs are urgently needed. Because the anthracyclines and mitoxantrone are quinones they are susceptible to reductive activation² by a variety of reducing enzymes to produce damaging reactive oxygen species leading to cardiotoxicity. The anthrapyrazoles are not quinones and cannot be

reductively activated. We previously showed³ in a structure-based 3D-QSAR study that a series of substituted anthrapyrazoles that we synthesized had potent cancer cell growth inhibitory effects. Following this we used molecular modeling to design and synthesize a series of bisanthrapyrazoles that contained a diester linkage joining two anthrapyrazoles together.⁴ However, the biological data on these bisanthrapyrazoles suggested that the ester linkages were susceptible to hydrolysis, possibly through the action of cellular esterases.⁴ We showed that these bisanthrapyrazoles had good cell growth inhibitory activity and the compounds with two or more methylene linkers formed bisintercalation complexes with DNA.⁴ In the present work we attempted to improve the stability of these compounds by replacing the ester linkage with the much more stable amide linkage (Fig. 1, compounds 1–5).

We previously showed that the strength of DNA binding for the anthrapyrazoles was strongly correlated with cell growth inhibition.³ Bisintercalators can potentially bind much more strongly than their analogous monointercalators because of the favorable entropic advantage that ensues after the binding of the first intercalating group. Because of their strong binding they should have a prolonged residence time on DNA⁵ allowing them to interfere with DNA pro-

* Corresponding author. Tel.: +1 204 474 8325; fax: +1 204 474 7617.

E-mail address: B_Hasinoff@UManitoba.ca (B.B. Hasinoff).

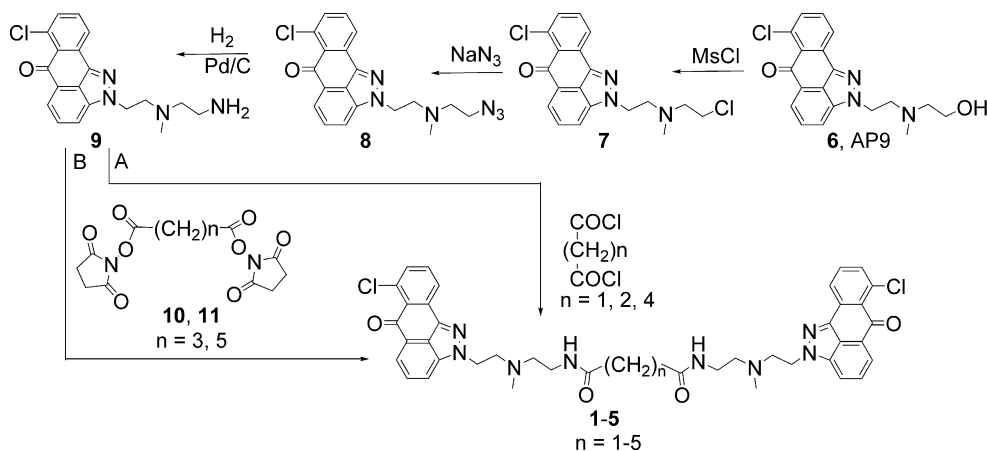


Figure 1. Reaction scheme and structures for the synthesis of the bisanthrapyrazoles **1**, **2**, **3**, **4**, and **5** ($n = 1-5$) starting from **6** (AP9). Compounds **1**, **2**, and **4** were prepared using Method A and compounds **3** and **5** were prepared using Method B as described in Section 4.

cessing enzymes. In principle, bisintercalators also should have enhanced DNA sequence specificity compared to monointercalators because monointercalators have the potential of binding to only 10 distinguishable sites, but for a binding site of 6 base pairs this increases to 2080 distinguishable sites.⁶ However, it should be noted, because the majority of intercalators, at best, show only a slight preference for GC base-pairs, sequence specificity may not necessarily be achieved by increasing the number of distinguishable sites. Bisintercalating compounds, as exemplified by echinomycin, occur naturally and it and several purely synthetic compounds have progressed into clinical trials as antitumor agents.^{5,7,8} In order to direct the synthesis of new bisanthrapyrazoles, molecular modeling and DNA docking studies were carried out on the amide-linked bisanthrapyrazoles containing different numbers of methylene linkers. Compound **6** (Fig. 1), which we previously had shown to have significant cell growth and topoisomerase II α inhibitory activity,^{3,4} was chosen as the scaffold for the synthesis of a series of the bisanthrapyrazole congeners. In addition to measuring the cell growth inhibitory effects of the bisanthrapyrazoles we also measured their ability to bind to DNA, to inhibit topoisomerase II α , and to cause topoisomerase II α -mediated DNA cleavage.

2. Results

2.1. Effect of the bisanthrapyrazoles on the thermal denaturation of DNA

The effects of 2 μM of the bisintercalators **1-5** and the monointercalator **6** on ΔT_m , the increase in the DNA thermal melt temper-

ature, of sonicated calf thymus DNA (5 $\mu\text{g}/\text{mL}$) are shown in Table 1. Doxorubicin (2 μM), which is a well known DNA intercalating drug, was used as a control and was observed to increase the T_m by 17.8 $^\circ\text{C}$ from 70.2 $^\circ\text{C}$. Compound **2** had the largest ΔT_m , and thus bound the strongest to DNA (Table 1 and Fig. 2). Compounds **2** and **3** both bound to DNA as or more strongly than doxorubicin, a well known DNA intercalator.⁹ The bisanthrapyrazoles **1**, **4**, and **5** all increased ΔT_m about the same as the parent **6**. In our previous study on the analogous ester-linked bisanthrapyrazoles⁴ we showed that the slope of a plot of ΔT_m versus drug concentration for a bisintercalator is approximately twice that of the monomeric monointercalator **6**. This is due to the bisintercalator occupying twice the number of intercalation sites on the DNA as had been previously shown from a comparison of the bisintercalator dye YOYO and its monomeric form YO-PRO.¹⁰ This is based on a simple model in which (1) the different intercalation sites contribute equally and independently to the free energy difference between the hybridized and melted states and (2) the presence of an intercalator at a site lowers the free energy of the hybridized state by a fixed, site-independent amount. Thus, the melting temperature of a DNA duplex should increase in proportion to the number of intercalated groups. The concentration dependence of ΔT_m for monomeric **6** (AP9) and the bisanthrapyrazoles **1-5** are shown in Figure 2A and the slopes of these plots are given in Figure 2B. A *t*-test comparison of the slopes showed that compounds **1**, **2**, and **3** had slopes that were significantly different ($p < 0.01$, < 0.001 , and < 0.001 , respectively) than monomer **6**. Compounds **4** and **5** did not yield slopes that were significantly different than monomer **6**. The ratio of the slopes of compounds **1-5** relative to that for **6** gave values of 1.7 ± 0.3 , 4.0 ± 0.8 , 3.4 ± 0.8 , 1.2 ± 0.2 , and 0.9 ± 0.2

Table 1
DNA ΔT_m , cell growth inhibition and topoisomerase II α inhibitory effects of the amide-linked bisanthrapyrazoles and their precursors

Compound	ΔT_m^a ($^\circ\text{C}$)	MTS cell growth inhibition		Resistance factor ^b	Topoisomerase II α inhibition IC ₅₀ (μM)
		K562 IC ₅₀ (μM)	K/VP.5 IC ₅₀ (μM)		
1	9.6	2.6	2.0	0.77	42
2	21.8	3.5	1.6	0.44	7
3	17.8	5.7	2.3	0.39	25
4	6.8	6.7	3.3	0.48	48
5	4.8	4.6	2.5	0.55	22
6 , AP9	5.4	3.1	1.9	0.63	10
8	1.1	3.6	ND	ND	25
9	10.2	3.6	1.5	0.43	18
Doxorubicin	17.8	0.3	0.5	1.81	ND

ND is not determined.

^a Experimental value at 2 μM .

^b The resistance factor was calculated from the ratio of the IC₅₀ value for the K/VP.5 cell line divided by that for the K562 cell line.

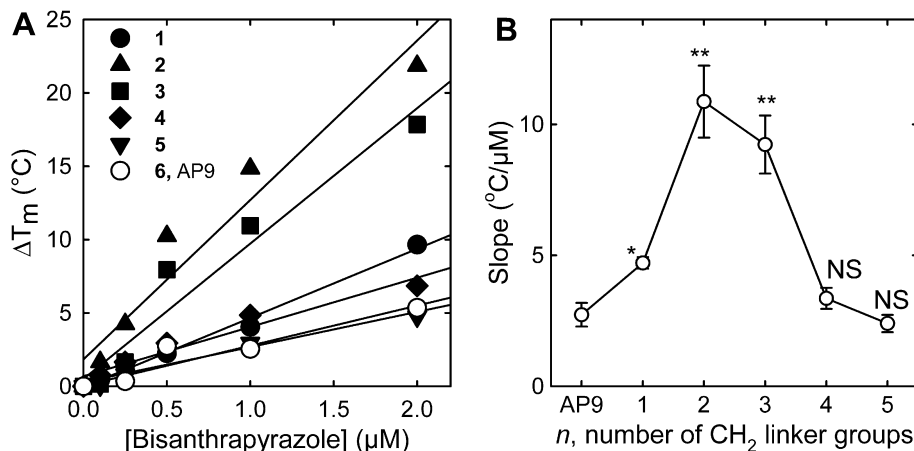


Figure 2. Concentration dependence of ΔT_m for the bisanthrapyrazoles binding to DNA. (A) Concentration dependence of ΔT_m for the bisanthrapyrazoles **1**, **2**, **3**, **4**, and **5** ($n = 1-5$) and parent monomer **6** for comparison. The solid straight lines are linear least squares calculated fits to the data. (B) Concentration dependence of the slopes \pm SEM calculated from the data in (A) (NS, not significant). The slopes of the plots in (A) for **1**, **2**, and **3** were all significantly different (*, **; $p < 0.01$, < 0.001 , respectively) than the parent **6**. Compounds with slopes approximately twice that of the parent monomer **6** indicate that they formed bisintercalation complexes with DNA.

where the SEMs were calculated from a propagation of errors analysis. The data were consistent with compounds **2** and **3** forming bisintercalating complexes. For compound **1** the data suggest a possible formation of a mixture of mono and bisintercalating complexes. This result differed from our previous study on the ester-linked bisanthrapyrazoles⁴ which showed that the compound with a single methylene linker did not bisintercalate into DNA. Compounds **4** and **5** gave ratios close to 1 indicating mono intercalation.

2.2. Effect of bisanthrapyrazoles on the decatenation activity of topoisomerase II α and on the stabilization of the covalent topoisomerase II α -DNA cleavable complex

Topoisomerase II alters DNA topology by catalyzing the passing of an intact DNA double helix through a transient double-stranded break made in a second helix and is critical for relieving torsional stress that occurs during replication and transcription and for daughter strand separation during mitosis.^{11,12} As shown in Table 1 all of the bisanthrapyrazoles inhibited the decatenation activity of human topoisomerase II α in the low micromolar concentration range. However, only **2**, which was the compound that bound the strongest to DNA, achieved a cytotoxic potency greater than that of the parent **6**. The decatenation assay is a measure of the ability of these compounds to inhibit the catalytic activity only, and is not a measure of whether these compounds acted as topoisomerase II poisons as do some widely used anticancer drugs.^{11,12} These include doxorubicin and the other anthracyclines, mitoxantrone, and etoposide.^{11,12} These and the anthrapyrazoles losoxantrone and piroxantrone,^{13,14} are thought to be cytotoxic by virtue of their ability to stabilize a covalent topoisomerase II-DNA intermediate (the cleavable complex). Stabilization of the covalent complex leads to double strand DNA breaks that are toxic to the cell. Thus, DNA cleavage assay experiments¹⁵ as we previously described^{3,4,16} were carried out using 50 μ M etoposide as a positive control to see whether 50 μ M of the test bisanthrapyrazoles stabilized the cleavable complex. As shown in Figure 3 the addition of etoposide (lane 10) to the reaction mixture containing topoisomerase II α and supercoiled pBR322 DNA induced formation of linear pBR322 DNA. Linear DNA was identified by comparison with linear pBR322 DNA produced by action of the restriction enzyme HindIII acting on a single site on pBR322 DNA (not shown). Based on integrated band intensities of linear DNA in Figure 3 none of the bisanthrapyrazoles (lanes 3–7) appeared to induce formation of

linear DNA comparable to that induced by etoposide (lane 10). If the bisanthrapyrazoles poison topoisomerase II α as we found with some of the anthrapyrazoles of our previous study,³ they do so at a level much lower than that of etoposide. As indicated by the absence of a relaxed DNA band, etoposide and all 5 bisanthrapyrazoles inhibited the relaxation of supercoiled pBR322 DNA by topoisomerase II α . These results indicate that, while etoposide both inhibited topoisomerase II α catalytic activity and induced DNA cleavage, the bisanthrapyrazoles acted primarily by inhibition of topoisomerase II α strand passage reactions. The ester-linked bisanthrapyrazoles of our previous study also did not induce significant DNA cleavage.⁴

2.3. Cell growth inhibitory effects of the bisanthrapyrazoles on human leukemia K562 cells and K/VP.5 cells with a decreased level of topoisomerase II α

As shown in Table 1 all of the bisanthrapyrazoles potentially inhibited the growth of K562 and K/VP.5 cells in the low micromolar range. These results suggest that the bisanthrapyrazoles were not too large or too charged to enter cells. In general, changing

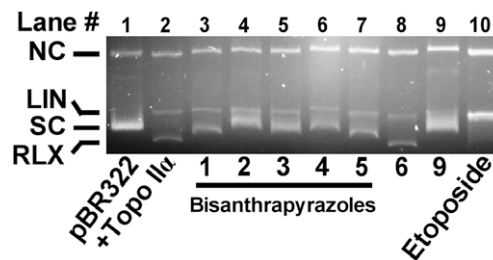


Figure 3. Effect of bisanthrapyrazoles **1**, **2**, **3**, **4**, and **5** and their monomeric precursors **6** and **9** on the topoisomerase II α -mediated relaxation and cleavage of 50 ng of supercoiled pBR322 plasmid DNA. This fluorescent image of the ethidium bromide-stained gel shows that topoisomerase II α (Topo II α) relaxed supercoiled (SC) pBR322 DNA (lane 1) to relaxed (RLX) DNA (lane 2). Topoisomerase II α was present in the reaction mixture for all lanes but lane 1. As shown in lane 10, etoposide treatment produced significant amounts of linear DNA (LIN). A small amount of nicked circular (NC) is normally present in the pBR322 DNA. A densitometric analysis of the linear DNA bands showed that all of the bisanthrapyrazoles produced much less linear DNA than the etoposide positive control (lane 10) did. The amount of linear DNA produced by the bisanthrapyrazoles was only slightly above control levels (lane 2). The concentration of all test compounds in the assay mixture was 50 μ M.

the number of methylene linkers did not produce a large effect on the inhibition of the growth of K562 cells as the IC_{50} values for compounds **1–5** varied only 2.6-fold.

Cancer cells can acquire resistance to topoisomerase II poisons by lowering their level and/or activity of topoisomerase II.^{11,17} Cells containing less topoisomerase II produce fewer DNA strand breaks in the presence of topoisomerase II poisons and are less cytotoxic. Thus, a resistant cell line may be used to test whether a drug that catalytically inhibits topoisomerase II might also act as a topoisomerase II poison.¹⁸ Conversely, a lack of change in sensitivity of a putative topoisomerase II poison to a cell line with a lowered topoisomerase II level can be taken to indicate that poisoning of topoisomerase II is not an important mechanism for a particular agent. We previously reported that topoisomerase II α and topoisomerase II β protein levels were reduced sixfold and threefold, respectively, in the K/VP.5 cell line with acquired resistance to etoposide compared with the parental K562 cells.^{19,20} As shown in Table 1 none of the bisanthrapyrazoles were cross resistant in K/VP.5 cells. The topoisomerase II poisons doxorubicin and mitoxantrone were 1.8–4.2-fold cross resistant, respectively. Thus both these results and the results of the cleavage assay (Fig. 3) suggest that the bisanthrapyrazoles do not inhibit cell growth by acting as topoisomerase II poisons.

2.4. Docking of the bisanthrapyrazoles into DNA

All five bisanthrapyrazoles docked into the DNA minor groove with similar configurations. All five also docked with both anthrapyrazole rings fully inserted into the doxorubicin intercalation sites with their aromatic rings highly coplanar with the DNA bases. An X-ray structure (PDB ID: 1DA9)⁹ of two molecules of doxorubicin separated by 4 base pairs bound to duplex DNA was used for the docking (Fig. 4). The structure of **2**, the bisanthrapyrazole that bound to DNA the strongest, docked into DNA is shown in Figure 4. An examination of the structure of **5** docked into DNA showed that the linker chain was longer than required which resulted in a slight bulge in the chain. The GOLDScores obtained from the docking are plotted as a function of n , the number of methylene linkers in Figure 5A. The bell-shaped plot showed a broad maximum with an n value in the 2–4 range suggesting that bisintercalation binding to DNA is predicted to be optimal in this range. The maximum value obtained from a quadratic fit (solid line) to the data indicated that an n value of 3.7 was optimal for binding to DNA. The experimentally determined strength of binding to DNA determined using ΔT_m as a measure is also shown plotted in Figure 5B as a function of n , the number of methylene linkers. The maximum in the quadratic fit (solid line) to the data in Figure 5B indicated that an n value of 2.6 was optimal for binding to DNA. Thus, the optimal number of methylene linkers calculated from the GOLD docking and the experimental number were in reasonably good agreement indicating that bisanthrapyrazole GOLD docking scores were a reasonable predictor of optimal linker length for strength of binding to DNA.

2.5. QSAR correlation analyses of GOLDScore, DNA binding affinity, K562 cell growth inhibition, and topoisomerase II α inhibition

A correlation analysis was carried out on the logarithm of the K562 IC_{50} values versus the GOLDScores and each of its component terms: (DNA–ligand hydrogen bond energy (external H-bond); DNA–ligand van der Waals (vdw) energy (external vdw); and the sum of the two ligand internal (vdw and torsion) terms as we previously described for a series of anthrapyrazoles.³ No significant correlation was found (all p values greater than 0.17). Likewise ΔT_m values were not significantly correlated with the GOLDScores

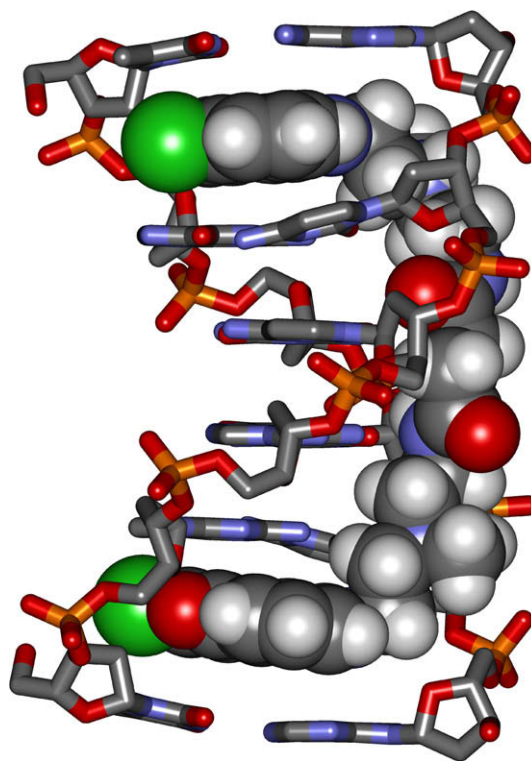


Figure 4. Docking of the protonated bisanthrapyrazole **2** into DNA. The highest scoring structure of the strongest DNA binding bisanthrapyrazole **2** (CPK structure) is shown docked into DNA (stick structure). The H-atoms of the DNA are not shown for clarity. The DNA structure is 1DA9 from the Protein Data Bank and is a DNA-(doxorubicin)₂ X-ray structure in which two doxorubicin molecules are bound to a 6-base pair piece of DNA.⁹ Both doxorubicin molecules were removed and **2** was docked into its place with the genetic algorithm docking program GOLD.

or any of its component terms. The logarithm of the K562 IC_{50} values versus ΔT_m were also not correlated (p of 0.9). In our previous study of a series of anthrapyrazoles that we synthesized, the logarithm of the K562 IC_{50} values and ΔT_m were highly correlated ($p < 0.0001$).³ The logarithm of the K562 IC_{50} data was also poorly correlated with the logarithm of the IC_{50} for the catalytic inhibition of topoisomerase II α ($p = 0.7$). The lack of correlation with the inhibition of topoisomerase II α activity IC_{50} does not necessarily indicate that these compounds lack activity as topoisomerase II poisons, rather they do not act through their inhibition of the catalytic activity of topoisomerase II α . Similarly, the logarithm of the IC_{50} for the catalytic inhibition of topoisomerase II α was also poorly (p of 0.14) correlated with ΔT_m . The lack of correlation is generally similar to what we found for our ester-linked bisanthrapyrazoles.⁴

3. Discussion

A series of amide-linked bisanthrapyrazoles based on the monomeric scaffold **6** with 1–5 methylene linkers, was synthesized in order to improve the potency and the stability of an earlier analogous series of ester-linked bisanthrapyrazoles we synthesized and characterized.⁴ In general, both neither K562 growth inhibitory effects nor inhibition of topoisomerase II α of the amide-linked bisanthrapyrazoles were significantly changed compared to the previous ester-linked bisanthrapyrazoles.⁴ As before⁴ molecular modeling and docking into DNA was used in order to determine the optimal linker length for optimal binding to DNA and selection for their subsequent synthesis. The concentration dependence of ΔT_m (Fig. 2B) for **2** and **3** were highly significantly increased over that of the parent **6**, a result which suggests that these two bis-

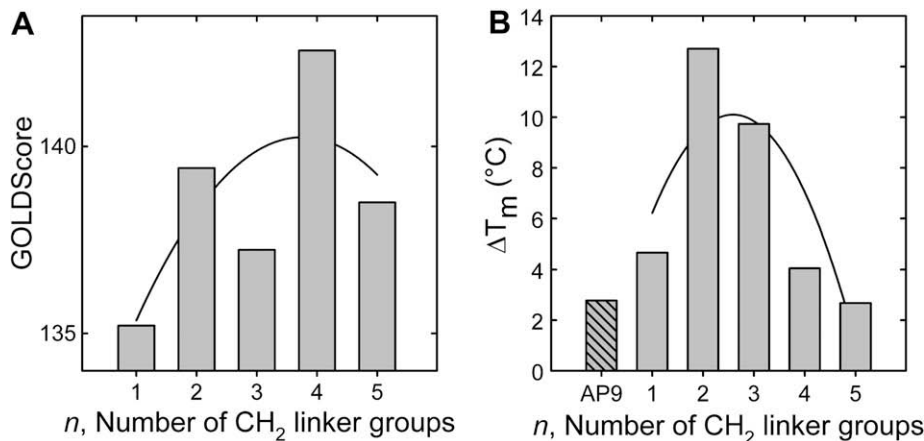


Figure 5. Calculated and experimental measures of binding of the bisanthrapyrazoles **1–5** binding to DNA. (A) GOLDScores obtained from the docking of the bisanthrapyrazoles into DNA as a function of n , the number of CH₂ linker groups in the bisanthrapyrazoles. The solid line is a quadratic fit of the GOLDScore values for the bisanthrapyrazoles with $n = 1–5$. (B) Experimentally measured ΔT_m values for the bisanthrapyrazoles with $n = 1–5$ and parent **6** (AP9) for comparison. The solid line is a quadratic fit of ΔT_m (solid line) for the bisanthrapyrazoles with $n = 1–5$.

anthrapyrazoles exclusively formed bisintercalation complexes with DNA. However, our docking results predicted that all of the compounds **1–5** should be able form bisintercalation complexes spanning 4 DNA base pairs. GOLDScores obtained from docking and the experimentally determined ΔT_m values both displayed broad maxima (Fig. 5) in the range of 2–4 methylene linkers. Thus, the calculated and experimental DNA binding affinities were in good agreement indicating that the docking was useful for selecting a range of optimal methylene linker lengths for synthesis. Though the bisanthrapyrazoles differed significantly in their ability to bind to DNA, this difference was not reflected in their ability to inhibit the growth of K562 cells. Thus, it can be concluded that while the design goal of increasing strength of DNA binding compared to monomer **6** through bisintercalation was achieved, the goal of increasing cell growth inhibition by changing the ester linkage to an amide linkage did not result in a significant improvement. Though the *in vitro* stability of the amide-linked bisanthrapyrazoles was not determined, it is likely that they are much more stable than the ester-linked bisanthrapyrazoles we previously described which should make the amide-linked bisanthrapyrazoles more efficacious as anticancer drugs.⁴ Future work will evaluate the stability, pharmacokinetics and antitumor efficacy of ester-linked bisanthrapyrazoles compared to the amide-linked bisanthrapyrazoles using a xenograft rodent model for human tumors.

The bisanthrapyrazoles **1–5** have a large number of rotatable bonds. The high degree of conformational flexibility of these molecules makes it computationally difficult to obtain the best possible GOLDScore. This likely explains the lack of a smooth change in GOLDScore as the number of linker groups was varied (Fig. 5A). Even so, the docking produced structurally reasonable bisintercalation complexes as shown by the example in Figure 4. Most of the driving force for binding is likely due to the high affinity that the anthrapyrazole rings have for the sites into which the bisanthrapyrazoles intercalate, thus anchoring the two ends of the bisanthrapyrazoles. DNA base pair specificity in bisanthrapyrazole binding to DNA may be another factor that contributes to GOLDScores lacking the power to accurately predict the strength of DNA binding. The bisanthrapyrazoles were docked into a single X-ray structure (PDB ID: 1DA9) which does not necessarily have the base pair sets which would lead to optimum binding to DNA.

Our previous study^{3,4} showed that **6** and the ester-linked bisanthrapyrazoles⁴ were strong topoisomerase II α inhibitors. As with the ester-linked bisanthrapyrazoles⁴ cell growth inhibition by

compounds **1–5** was not correlated with inhibition of topoisomerase II α -mediated catalytic decatenation activity. This result indicates that the catalytic inhibition of topoisomerase II was not the primary mechanism by which these compounds inhibited cell growth. Compounds **1–5** did not significantly induce formation of linear DNA through stabilization of a covalent topoisomerase II α -DNA cleavable complex in the DNA cleavage assay. These results are in contrast to our previously described⁴ results that showed the ester-linked bisanthrapyrazoles did have some topoisomerase II poisoning activity. Also, several of the monomeric anthrapyrazoles we previously studied³ did induce formation of linear DNA. The bisanthrapyrazoles may also target other DNA processing enzymes due to their ability to bisintercalate into DNA.

In summary, a series of amide-linked bisanthrapyrazoles were designed to bisintercalate into DNA using molecular modeling and docking. As predicted from the docking results, bisanthrapyrazoles with more than one methylene linker formed bisintercalation complexes with DNA and significantly inhibited K562 cell growth.

4. Experimental

4.1. Biological assays

4.1.1. Materials, cell culture, and growth inhibition assays

The plasmid DNA and the absorbance-based cell proliferation assay and other materials were as previously described.⁴ The human leukemia K562 cells, obtained from the American Type Culture Collection and K/VP.5 cells (a 26-fold etoposide-resistant K562-derived sub-line with decreased levels of topoisomerase II α mRNA and protein)¹⁷ were maintained as suspension cultures as described.⁴ The IC₅₀ values for growth inhibition in the cell growth inhibition and decatenation assays were measured by fitting the absorbance- or fluorescence-drug concentration data, respectively, to a four-parameter logistic equation as described.⁴ Errors, where quoted, are SEMs.

4.1.2. Topoisomerase II α kDNA decatenation and pBR322 DNA relaxation and cleavage assays

The fluorescence plate reader based spectrofluorometric decatenation assay we developed was used to determine the catalytic inhibition of topoisomerase II α .^{4,18} kDNA which consists of highly catenated networks of circular DNA is decatenated by topoisomer-

ase II α in an ATP-dependent reaction to yield individual minicircles of DNA. The assay conditions and the expression, extraction and purification of recombinant full-length human topoisomerase II α were previously described.^{4,18} Topoisomerase II-cleaved DNA complexes produced by anticancer drugs may be trapped by rapidly denaturing the complexed enzyme with sodium dodecyl sulfate (SDS).^{3,15} The drug-induced cleavage of double-stranded closed circular pBR322 DNA to form linear DNA at 37 °C was followed by separating the SDS-treated reaction products using ethidium bromide gel electrophoresis essentially as described, except that all components of the assay mixture were assembled and mixed on ice prior to addition of the drug.^{4,15} This greatly increased the amount of linear DNA produced, and thus increased the sensitivity of the assay.

4.1.3. Thermal denaturation of DNA assay

Compounds that intercalate into DNA stabilize the DNA double helix and increase the temperature at which the DNA denatures or unwinds.^{21–23} The effect of 0.1–2 μ M anthrapyrazole or bisanthrapyrazole on the increase in the ΔT_m of sonicated calf thymus DNA (5 μ g/mL) was measured in 10 mM Tris–HCl buffer (pH 7.4) in a Cary 1 (Varian, Mississauga, Canada) double beam spectrophotometer by measuring the absorbance increase at 260 nm upon the application of a temperature ramp of 1 °C/min as we previously described.^{3,4} Doxorubicin (2 μ M), which is a strong DNA intercalator, was used as a positive control.^{3,4} The slopes of the plots for monomer **6** were compared to those of the bisanthrapyrazoles **1–5** using a *t*-test comparison of the slopes.²⁴

4.2. Molecular modeling and docking

4.2.1. Docking of the bisanthrapyrazoles into an X-ray structure of DNA

All molecular modeling was done using SYBYL 7.3²⁵ on a PC workstation with a Redhat Enterprise 4 Linux operating system. All molecules except the DNA were built using SYBYL and geometry optimized with the Tripos force field. The protonated bisanthrapyrazoles were docked into the doxorubicin binding site of a 6-base pair X-ray crystal structure of 2 molecules of doxorubicin bound to double stranded DNA, d(TGGCCA)/doxorubicin, (<http://www.rcsb.org/pdb/>; PDB ID: 1DA9)⁹ using the genetic algorithm docking program GOLD version 3.2²⁶ with default GOLD parameters and atom types and with 500 starting runs²⁷ as we described.⁴ GOLDScore was used as the fitness function with flipping options of planar and pyramidal nitrogens being allowed. The top 10 structures were then re-scored using a local optimization (simplexing) to obtain the final GOLDScore. Rescoring did not affect the initial relative scoring order. The two doxorubicin molecules in the 1DA9 DNA X-ray structure are separated by four intervening base pairs. The first and second base pairs buckle out to accommodate the bound doxorubicin in this structure.⁹ The DNA structure was prepared by removing both of the bound doxorubicin and water molecules to avoid potential interference with the docking. Hydrogens were added to the DNA with the SYBYL Biopolymer module. The binding site (6 Å) was defined using a previously docked ester-linked bisanthrapyrazole in the minor groove.⁴ Doxorubicin docked back into the DNA structure with a heavy atom root-mean-squared distance of 1.3 Å compared to the X-ray structure.⁹ The graphic was prepared with DS Visualizer 2.0 (Accelrys, San Diego, CA).

4.3. Chemistry

4.3.1. General

¹H and ¹³C nuclear magnetic resonance (NMR) spectra were recorded at 300 K in 5 mm NMR tubes on a Bruker Avance 300 MHz NMR spectrometer operating at 300.13 MHz for ¹H NMR and

75.5 MHz for ¹³C NMR, respectively, in chloroform-*d*, unless otherwise indicated. Chemical shifts are given in parts per million (ppm) (+/– 0.01 ppm) relative to tetramethylsilane (0.00 ppm) in the case of the ¹H NMR spectra, and to the central line of CDCl₃ (δ 77.0) for the ¹³C NMR spectra. Melting points were taken on an Electrothermal (England) melting point apparatus and were uncorrected. The high resolution mass spectra were run on an Agilent 6210 Accurate-Mass Time-of-Flight (TOF) LC/MS system (Agilent Technologies, Mississauga, Canada) using electrospray ionization. The samples were dissolved in methanol and were infused into the mass spectrometer with an Agilent 1200 HPLC using acetonitrile/water containing 0.1% (v/v) formic acid as the mobile phase. The silica gel (SiGel, 230–400 mesh ultrapure) was obtained from Silicycle (Quebec, Canada). The alumina (aluminum oxide, activated, basic, Brockmann I, standard grade, ~150 mesh) was obtained from Fisher (Ottawa, Canada). TLC was performed on plastic-backed plates bearing 200 μ m Silica Gel 60 F₂₅₄ (Silicycle). Compounds were visualized by quenching of fluorescence by UV light (254 nm) where applicable. The reaction conditions were not optimized for reaction yields. Dichloromethane and triethylamine were refluxed over calcium hydride and distilled. Compound **6** (AP9) (7-chloro-2-[2-[(2-hydroxyethyl)methylamino]ethyl]anthra[1,9-*cd*]pyrazol-6(2*H*)-one) was prepared from 1,5-dichloroanthraquinone as we previously described.³

4.3.2. General procedure for the synthesis of the bisanthrapyrazoles

The amide-linked bisanthrapyrazoles **1**, **2**, and **4** were prepared by the reaction of **9** with the corresponding acid chlorides in dichloromethane. Compounds **3** and **5** were prepared by the reaction of **9** with the corresponding bis-*N*-hydroxysuccinimide esters in dichloromethane. Method A for the synthesis of **1**, **2**, and **4** was as follows. The acid chlorides (0.28 mmol, 0.5 equiv) were added slowly to a clear orange-red solution of **9** (200 mg, 0.564 mmol) in dichloromethane (3 mL). A light orange precipitate formed immediately. Ether (3 mL) was added with overnight stirring. The mixture was centrifuged and the solid was twice washed with ether and dried. The solid was extracted into chloroform/aqueous NaOH and dried over Na₂SO₄. The solvent was removed with a vacuum pump. We found that the reaction of **9** with the acid chlorides gave low yields because the HCl produced in the reaction caused **9** to precipitate as the HCl salt. It was for this reason that **3** and **5** were prepared using Method B. Method B for the synthesis of **3** and **5** was as follows. *N*-Hydroxysuccinimide ester **10** or **11** (0.14 mmol, 0.5 equiv) was treated with **9** (100 mg, 0.282 mmol) in dichloromethane (5 mL). The mixture was stirred overnight and the solvent was removed under reduced pressure. In general, the free base bisanthrapyrazoles formed sticky films. These could be precipitated into easily handled powders by dissolving the oily amides in dichloromethane and then adding hexane.

4.3.2.1. 7-Chloro-2-[2-[(2-chloroethyl)methylamino]ethyl]anthra[1,9-*cd*]pyrazol-6(2*H*)-one (7**).** Mesyl chloride (1.74 mL, 22.5 mmol) and triethylamine (3.13 mL, 22.5 mmol) were added to a solution of **6** (AP9, 2.0 g, 5.62 mmol) in chloroform (30 mL) on ice. The mixture was stirred overnight under nitrogen. The product was extracted into chloroform/aqueous sodium hydroxide, and the chloroform phase was dried over Na₂SO₄. The solvent was removed, affording crude **7**, 2.07 g as yellow crystals. This reaction afforded the chloroethyl derivative rather than the expected mesylate, presumably via a reactive aziridine intermediate. The crude product was purified by silica gel column chromatography (ethyl acetate as eluant), affording 1.82 g (0.487 mmol) in 86% yield; mp: 144–146 °C; ¹H NMR (CDCl₃) δ 8.20 (dd, 1H); 7.99 (d, 1H); 7.73–7.53 (m, 4H); 4.61 (t, 2H); 3.43 (t, 2H); 3.09 (t, 2H); 2.79 (t, 2H); 2.39 (s, 3H). ¹³C NMR (CDCl₃) δ

~183; 139.3; 137.2; 134.7; 132.9; 132.6; 129.1; 128.7; 126.9; 121.8; 121.0; 114.9; 59.2; 57.1; 48.4; 42.4; 41.2; HRMS (ESI), m/z (M+H)⁺: calcd 374.0827, obsd 374.0819. The chloride **7** was quite reactive and reacted smoothly with sodium azide affording the azide **8** in high yield.

4.3.2.2. 7-Chloro-[2-[(2-azidoethyl)methylamino]ethyl]anthra-[1,9-cd]pyrazol-6(2H)-one (8). Compound **7** (1.10 g, 2.54 mmol) was added to sodium azide (1.65 g, 25.4 mmol) in dimethylformamide (10 mL) and the mixture was heated at 60 °C under nitrogen for 24 h. The solution was cooled to room temperature, added to water (100 mL), and stirred for 30 min. The precipitate was filtered affording 0.88 g (2.31 mmol) in 91% yield; mp: 101–102 °C; ¹H NMR (CDCl₃) δ 8.20 (dd, 1H); 8.00 (d, 1H); 7.74–7.52 (m, 4H); 4.62 (t, 2H); 3.23 (t, 2H); 3.08 (t, 2H); 2.66 (t, 2H); 2.39 (s, 3H). ¹³C NMR (CDCl₃) δ 182.6; 139.3; 137.2; 134.7; 132.9; 132.5; 128.6; 126.9; 122.7; 121.8; 120.9; 114.7; 57.2; 56.8; 48.9; 48.5; 42.4; HRMS (ESI), m/z (M+H)⁺: calcd 381.1230, obsd 381.1220. The product was pure enough to be used directly in the next step.

4.3.2.3. 7-Chloro-[2-[(2-aminoethyl)methylamino]ethyl]anthra-[1,9-cd]pyrazol-6(2H)-one (9). Compound **8** (300 mg, 0.789 mmol) was dissolved in methanol (80 mL) containing HCl (1.80 mmol). Palladium on charcoal (60 mg, 10% Pd, 0.056 mmol) was added and the mixture was placed under a positive hydrogen atmosphere for 2 h. The mixture was then filtered through a Celite pad. The methanol filtrate was condensed, extracted into chloroform/aqueous sodium hydroxide, the chloroform phase dried over Na₂SO₄, condensed, and dried on a vacuum pump, affording 238 mg (0.672 mmol) of crude **9** as a yellow solid in 85% yield; ¹H NMR (CDCl₃) δ 8.202 (dd, 1H); 7.99 (d, 1H); 7.70–7.54 (m, 4H); 4.61 (t, 2H); 3.01 (t, 2H); 2.65 (t, 2H); 2.48 (t, 2H); 2.34 (s, 3H). ¹³C NMR (CDCl₃) δ 182.8; 139.4; 138.4; 138.2; 137.3; 134.7; 133.0; 132.6; 129.1; 128.7; 126.8; 122.7; 121.8; 121.0; 114.8; 60.68; 57.5; 48.5; 42.4; HRMS (ESI), m/z (M+H)⁺: calcd 355.1325, obsd 355.1317. The product was pure enough to be used directly in the next step.

4.3.2.4. 1-({5-[(2,5-Dioxo-1-pyrrolidinyl)oxy]-5-oxopentanoyl}-oxy)-2,5-pyrrolidone (10). Compound **10** was prepared as described.²⁸ Mp: 128–130 °C (lit. 129–131 °C). The NMR matched that reported.

4.3.2.5. 1-({7-[(2,5-Dioxo-1-pyrrolidinyl)oxy]-7-oxoheptanoyl}-oxy)-2,5-pyrrolidone (11). *N*-Hydroxysuccinimide (1.27 g; 11.0 mmol), tetrahydrofuran (30 mL), and triethylamine (1.11 g, 1.52 mL; 11.0 mmol) were added into a 100 mL round bottom flask. After the mixture was cooled to 0 °C, pimeloyl chloride (0.8 mL, 0.985 g, 5.0 mmol) was slowly added. The mixture was stirred for 2 h at room temperature. The solvent was removed and the residue was dissolved in dichloromethane (100 mL) and washed with water (3 × 50 mL) and dried over Na₂SO₄. An off-white solid was obtained after filtration and evaporation of solvent. Recrystallization from isopropyl alcohol yielded a white solid (1.6 g, 90%); mp: 146–148 °C; ¹H NMR (300 MHz, CDCl₃) δ 2.82 (s, 8H); 2.63 (t, *J* = 7.3 Hz, 4H); 1.74–1.84 (m, 4H); 1.47–1.60 (m, 4H); ¹³C NMR (75.5 MHz, CDCl₃) δ 169.1, 168.4, 30.7, 27.8, 25.6, 24.1; HRMS (ESI), m/z (M+H)⁺: calcd 355.1141, obsd 355.1131.

4.3.2.6. *N,N*-Bis(2-((2-(7-chloro-6-oxo-6H-dibenzo[cd,g]indazol-2-yl)ethyl)methylamino)ethyl) malonamide (1). Compound **9** (200 mg, 0.564 mmol) was treated with malonyl chloride (27.4 μL, 40.0 mg, 0.282 mmol) according to Method A affording **1** as an orange solid. The crude product was purified by alumina column chromatography using chloroform/methanol 20:1 and then 10:1 as eluants. Yield 25 mg (11%); mp: 105–108 °C; ¹H NMR δ 8.07 (dd, *J*₁ = 7.0 Hz, *J*₂ = 1.9 Hz, 2H, ArH), 7.87 (d, *J* = 7.0 Hz, 2H, ArH), 7.70–7.46 (m, 8H,

ArH), 6.85 (t, *J* = 4.6 Hz, 2H, amide NH), 4.54 (t, 4H, *J* = 6.3 Hz, NNCH₂), 3.18 (q, 4H, *J* = 5.5 Hz), 2.98 (t, *J* = 6.3 Hz, 4H, NNCH₂CH₂), 2.68 (s, 2H COCH₂CO), 2.52 (t, *J* = 5.5 Hz, 4H), 2.30 (s, 6H, 2 × NCH₃); ¹³C NMR δ 182.4, 166.8, 139.1, 138.1, 137.1, 134.5, 132.9, 132.5, 128.9, 128.6, 126.8, 122.9, 121.8, 120.9, 114.7, 56.9, 56.2, 48.3, 42.7, 42.2, 36.9; HRMS (ESI), m/z (M+H)⁺: calcd 777.2471, obsd 777.2468.

4.3.2.7. *N,N*-Bis(2-((2-(7-chloro-6-oxo-6H-dibenzo[cd,g]indazol-2-yl)ethyl)methylamino)ethyl) succinamide (2). Compound **9** (200 mg, 0.564 mmol) was treated with succinyl chloride (31.04 μL, 43.7 mg, 0.282 mmol) according to Method A affording **2** as an orange solid. The product was separated on a short silica gel column. The crude product was purified by silica gel column chromatography using chloroform/methanol 9:1 as eluant. Yield 25 mg (11%); mp: 138–140 °C; ¹H NMR δ 8.16 (dd, 2H); 7.95 (d, 2H); 7.60 (m, 8H); 5.86 (t, 2H); 4.58 (t, 4H); 3.16 (q, 4H); 3.00 (t, 4H); 2.51 (t, 4H); 2.33 (s, 6H); 2.00 (s, 4H); ¹³C NMR δ 182.6, 171.7, 139.3, 138.3, 137.2, 134.6, 133.0, 132.6, 129.1, 128.8, 127.0, 122.6, 121.7, 121.0, 114.7, 57.1, 56.4, 48.4, 42.2, 36.7, 31.1; HRMS (ESI), m/z (M+H)⁺: calcd 791.2627, obsd 791.2593.

4.3.2.8. *N,N*-Bis(2-((2-(7-chloro-6-oxo-6H-dibenzo[cd,g]indazol-2-yl)ethyl)methylamino)ethyl) glutaramide (3). Compound **9** (100 mg, 0.282 mmol) was treated with **10** (45.6 mg, 0.14 mmol) according to Method B affording **3** as an orange solid. The crude product was purified as for **1**. Yield 60 mg (53%); mp: 130–133 °C; ¹H NMR (300 MHz, CDCl₃) δ 8.12 (dd, *J*₁ = 7.3 Hz, *J*₂ = 1.8 Hz, 2H, ArH), 7.90 (d, *J* = 7.3 Hz, 2H, ArH), 7.70–7.46 (m, 8H, ArH), 5.72 (s, br, 2H, amide NH), 4.59 (t, 4H, *J* = 6.0 Hz, NNCH₂), 3.18 (q, 4H, *J* = 5.4 Hz), 3.02 (t, *J* = 6.0 Hz, 4H, NNCH₂CH₂), 2.52 (t, *J* = 5.4 Hz, 4H), 2.35 (s, 6H, 2 × NCH₃), 2.01 (t, *J* = 6.4 Hz, 4H, 2 × COCH₂), 1.56–1.50 (m, 2H, COCH₂CH₂); ¹³C NMR (75.5 MHz, CDCl₃) δ 182.5, 172.1, 139.3, 138.1, 137.1, 134.6, 133.0, 132.6, 129.0, 128.7, 126.9, 122.5, 121.8, 120.9, 114.8, 56.9, 56.5, 48.2, 42.0, 36.5, 35.2, 21.5; HRMS (ESI), m/z (M+H)⁺: calcd 805.2784, obsd 805.2784.

4.3.2.9. *N,N*-Bis(2-((2-(7-chloro-6-oxo-6H-dibenzo[cd,g]indazol-2-yl)ethyl)methylamino)ethyl) adipamide (4). Adipoyl chloride (41.8 μL, 51.6 mg, 0.282 mmol) was added to a solution of **9** (200 mg, 0.564 mmol) in dichloromethane at 0 °C. A yellow precipitate formed. The reaction mixture was stirred overnight at room temperature and was then centrifuged. The supernatant was removed and the solid was recrystallized twice in methanol/ether. The solid was then extracted into chloroform/aqueous NaOH and dried over Na₂SO₄. Compound **4** was afforded as an orange solid after the solvent was removed by a vacuum pump. The crude product was purified as for **1**. Yield 15 mg (6%); mp: 110–114 °C; ¹H NMR δ 8.11 (dd, *J*₁ = 7.1 Hz, *J*₂ = 2.0 Hz, 2H, ArH), 7.90 (d, *J* = 7.1 Hz, 2H, ArH), 7.68–7.45 (m, 8H, ArH), 5.71 (t, *J* = 4.9, 2H, amide NH), 4.59 (t, 4H, *J* = 6.0 Hz, NNCH₂), 3.18 (q, 4H, *J* = 5.7 Hz), 3.02 (t, *J* = 6.0 Hz, 4H, NNCH₂CH₂), 2.53 (t, *J* = 5.7 Hz, 4H), 2.36 (s, 6H, 2 × NCH₃), 1.54 (t, *J* = 6.5 Hz, 4H, 2 × COCH₂), 1.25 (t, *J* = 6.5 Hz, 4H, COCH₂CH₂); ¹³C NMR δ 182.5, 172.5, 139.4, 138.1, 137.1, 134.6, 133.1, 132.6, 128.8, 128.6, 126.7, 122.4, 121.8, 120.9, 114.8, 56.9, 56.6, 48.2, 42.0, 36.5, 35.8, 22.6; HRMS (ESI), m/z (M+H)⁺: calcd 819.2940, obsd 819.2925.

4.3.2.10. *N,N*-Bis(2-((2-(7-chloro-6-oxo-6H-dibenzo[cd,g]indazol-2-yl)ethyl)methylamino)ethyl) pimelamide (5). Compound **9** (100 mg, 0.282 mmol) was treated with **11** (49.5 mg, 0.14 mmol) according to Method B affording **5** as an orange solid. The crude product was purified as for **1**. Yield 81 mg (69%); mp: 110–113 °C; ¹H NMR (300 MHz, CDCl₃) δ 8.07 (dd, *J*₁ = 7.0 Hz, *J*₂ = 2.0 Hz, 2H, ArH), 7.83 (d, *J* = 7.0 Hz, 2H, ArH), 7.65–7.44 (m, 8H, ArH), 5.60 (t, *J* = 4.7 Hz, 2H, amide NH), 4.56 (t, 4H, *J* = 6.0 Hz,

NNCH₂), 3.16 (q, 4H, *J* = 5.7 Hz), 3.00 (t, *J* = 6.0 Hz, 4H, NNCH₂CH₂), 2.50 (t, *J* = 5.7 Hz, 4H), 2.34 (s, 6H, NCH₃), 1.58 (t, *J* = 7.6 Hz, 4H, COCH₂), 1.24–1.14 (m, 4H, COCH₂CH₂), 0.91–0.81 (m, 2H, COCH₂CH₂CH₂); ¹³C NMR (75.5 MHz, CDCl₃) δ 183.2, 172.8, 139.3, 138.0, 137.0, 134.5, 133.0, 132.5, 128.8, 128.7, 126.7, 122.4, 121.8, 120.9, 114.8, 56.8, 56.6, 48.1, 41.9, 36.5, 36.1, 28.7, 25.1; HRMS (ESI), *m/z* (M+H)⁺: calcd 833.3097, obsd 833.3077.

Acknowledgments

Supported by grants from the Canadian Institutes of Health Research, the Canada Research Chairs Program, a Canada Research Chair in Drug Development to Brian Hasinoff, the Robert A. Welch Foundation (Grant AF-0005), the Herbert and Kate Dishman Endowment at Southwestern University to Frank Guziec and NIH grant CA90787 to Jack Yalowich.

Supplementary data

Supplementary data associated with this article can be found in the online version, at doi:10.1016/j.bmc.2009.04.072.

References and notes

- Corbett, A. H.; Osheroff, N. *Chem. Res. Toxicol.* **1993**, *6*, 585.
- Maliszka, K. L.; Hasinoff, B. B. *Arch. Biochem. Biophys.* **1995**, *321*, 51.
- Liang, H.; Wu, X.; Guziec, L. J.; Guziec, F. S., Jr.; Larson, K. K.; Lang, J.; Yalowich, J. C.; Hasinoff, B. B. *J. Chem. Inf. Model.* **2006**, *46*, 1827.
- Hasinoff, B. B.; Liang, H.; Wu, X.; Guziec, L. J.; Guziec, F. S., Jr.; Yalowich, J. C. *Bioorg. Med. Chem.* **2008**, *16*, 3959.
- Antonini, I.; Santoni, G.; Lucciarini, R.; Amantini, C.; Sparapani, S.; Magnano, A. *J. Med. Chem.* **2006**, *49*, 7198.
- Gago, F. *Methods* **1998**, *14*, 277.
- Dawson, S.; Malkinson, J. P.; Paumier, D.; Searcey, M. *Nat. Prod. Rep.* **2007**, *24*, 109.
- Martinez, R.; Chacon-Garcia, L. *Curr. Med. Chem.* **2005**, *12*, 127.
- Leonard, G. A.; Hambley, T. W.; McAuley-Hecht, K.; Brown, T.; Hunter, W. N. *Acta Crystallogr. D. Biol. Crystallogr.* **1993**, *49*, 458.
- Bjorndal, M. T.; Fygenon, D. K. *Biopolymers* **2002**, *65*, 40.
- Fortune, J. M.; Osheroff, N. *Prog. Nucleic Acid Res. Mol. Biol.* **2000**, *64*, 221.
- Li, T. K.; Liu, L. F. *Annu. Rev. Pharmacol. Toxicol.* **2001**, *41*, 53.
- Leteurtre, F.; Kohlhagen, G.; Paul, K. D.; Pommier, Y. *J. Natl. Cancer Inst.* **1994**, *86*, 1239.
- Capranico, G.; Palumbo, M.; Tinelli, S.; Mabilia, M.; Pozzan, A.; Zunino, F. *J. Mol. Biol.* **1994**, *28*, 1218.
- Burden, D. A.; Froelich-Ammon, S. J.; Osheroff, N. *Methods Mol. Biol.* **2001**, *95*, 283.
- Hasinoff, B. B.; Wu, X.; Begleiter, A.; Guziec, L.; Guziec, F. S., Jr.; Giorgianni, A.; Yang, S.; Jiang, Y.; Yalowich, J. C. *Cancer Chemother. Pharmacol.* **2006**, *57*, 221.
- Fattman, C.; Allan, W. P.; Hasinoff, B. B.; Yalowich, J. C. *Biochem. Pharmacol.* **1996**, *52*, 635.
- Hasinoff, B. B.; Wu, X.; Krokhin, O. V.; Ens, W.; Standing, K. G.; Nitiss, J. L.; Sivaram, T.; Giorgianni, A.; Yang, S.; Jiang, Y.; Yalowich, J. C. *Mol. Pharmacol.* **2005**, *67*, 937.
- Ritke, M. K.; Allan, W. P.; Fattman, C.; Gunduz, N. N.; Yalowich, J. C. *Mol. Pharmacol.* **1994**, *46*, 58.
- Ritke, M. K.; Roberts, D.; Allan, W. P.; Raymond, J.; Bergoltz, V. V.; Yalowich, J. C. *Br. J. Cancer* **1994**, *69*, 687.
- Sissi, C.; Leo, E.; Moro, S.; Capranico, G.; Mancia, A.; Menta, E.; Krapcho, A. P.; Palumbo, M. *Biochem. Pharmacol.* **2004**, *67*, 631.
- Priebe, W.; Fokt, I.; Przewloka, T.; Chaires, J. B.; Portugal, J.; Trent, J. O. *Methods Enzymol.* **2001**, *340*, 529.
- McGhee, J. D. *Biopolymers* **1976**, *15*, 1345.
- Jones, D. *Pharmaceutical Statistics*; Pharmaceutical Press: London, 2002.
- SYBYL 7.3, Tripos, 1699 South Hanley Rd., St. Louis, MO, 63144, USA, 2008.
- GOLD 3.2, CCDC Software Ltd, Cambridge, UK, 2008.
- Verdonk, M. L.; Cole, J. C.; Hartshorn, M. J.; Murray, C. W.; Taylor, R. D. *Proteins* **2003**, *52*, 609.
- van den Berg, T. A.; Feringa, B. L.; Roelfes, G. *Chem. Commun.* **2007**, 180.